Separation Science and Technology
Publication details, including instructions for authors and subscription information:
http://www.informaworld.com/smpp/title~content=t713708471

Fouling Layer with Fractionated Extracellular Polymeric Substances of Activated Sludge

Guang-Hui Yu[a]; Duu-Jong Lee[b]; Pin-Jing He[a]; Li-Ming Shao[a]; Juin-Yih Lai[c]
[a] College of Environmental Science & Engineering, Key Laboratory of Yangtze River Water Environment, State Key Laboratory of Pollution Control & Resources Reuse, Tongji University, Shanghai, China [b] Department of Chemical Engineering, National Taiwan University, Taipei, Taiwan [c] Center of Membrane Technology, Department of Chemical Engineering, Chung Yuan Christian University, Chungli, Taiwan

Online publication date: 23 April 2010

To cite this Article Yu, Guang-Hui , Lee, Duu-Jong , He, Pin-Jing , Shao, Li-Ming and Lai, Juin-Yih(2010) 'Fouling Layer with Fractionated Extracellular Polymeric Substances of Activated Sludge', Separation Science and Technology, 45: 7, 993 — 1002
To link to this Article: DOI: 10.1080/01496391003666213
URL: http://dx.doi.org/10.1080/01496391003666213

Separation Science and Technology, 45: 993–1002, 2010

ISSN: 0149-6395 print/1520-5754 online
DOI: 10.1080/01496391003666213

Taylor & Francis
Taylor & Francis Group

Fouling Layer with Fractionated Extracellular Polymeric Substances of Activated Sludge

Guang-Hui Yu,[1] Duu-Jong Lee,[2] Pin-Jing He,[1] Li-Ming Shao,[1] and Juin-Yih Lai[3]

[1]*College of Environmental Science & Engineering, Key Laboratory of Yangtze River Water Environment, State Key Laboratory of Pollution Control & Resources Reuse, Tongji University, Shanghai, China*

[2]*Department of Chemical Engineering, National Taiwan University, Taipei, Taiwan*

[3]*Center of Membrane Technology, Department of Chemical Engineering, Chung Yuan Christian University, Chungli, Taiwan*

The soluble microbial products (SMP) and extracellular polymeric substances (EPS) significantly affect fouling in membrane filtration. This work filtered SMP and fractionated EPS of activated sludge using a 0.45 mm filter membrane. The fluorescently labeled stains and confocol laser scanning microscopy (CLSM) images *in situ* visualized the distributions of proteins, α-polysaccharides, β-polysaccharides, lipids, total cells, and dead cells of different EPS fractions in the fouling layers. The role of individual SMP and fractionated EPS fractions on membrane fouling was discussed.

Keywords confocal laser scanning microscopy; extracellular polymeric substances; filterability; fluorescence staining; sludge

INTRODUCTION

Membrane separation presents a widely adopted nonthermal dehydration means in chemical and pharmaceutical industries (1–4). Fast filtration with minimum irreversible membrane fouling is desired (5–15). Membrane fouling results in flux decline and increases pressure drop across the membrane (16,17). Reviews for membrane fouling are available in (16,18–23).

The soluble microbial products (SMP), extracellular polymeric substances (EPS), and biopolymer clusters (BPC) play a crucial role in membrane fouling (24–27). Wisniewski and Grasmick (28) claimed that soluble constituents in mixed liquor contributed >52% of the total resistance of membrane filtration. Bouhabila et al. (29) reported that the colloids fraction was the major foulant on membrane. Defrance et al. (30) noted that the suspended solids are the key foulant of MBR. Bouhabila et al. (31) concluded that the colloids are the main foulant of membrane. Protein and polysaccharides have been identified as the major organic foulants (32–35). Ramesh et al. (36,37) revealed the potentials of individual components in EPS to foul the MBR membrane.

The characteristics of EPS of sludge suspensions play a predominant role in determining sludge dewaterability (38,39). The total quantity of EPS (40) and the quantities of proteins (41) or polysaccharides (42) affect sludge dewaterability. Yu et al. (38) developed an EPS fractionation approach and demonstrated that the proteins and the proteins/polysaccharides ratio in the supernatant and slime fractions, which were usually decanted due to their assumed lower content of organic matters, markedly impact sludge dewaterability. Direct observation of the deposit patterns of each component of the EPS provides in-depth understanding on how the membrane should interact with those organic substances (43).

This study first fractionated the total EPS of activated sludge into supernatant, slime, loosely bound-EPS (LB-EPS), and tightly bound-EPS (TB-EPS) fractions using approaches refined from that used by Yu et al. (38). The acquired EPS fractions after removal of cells were individually filtered using MF membrane in dead-end mode. The objectives of this study were

i. to apply the fluorescently labeled stains combining with CLSM images to in situ visualize the distribution patterns of proteins, α-polysaccharides, β-polysaccharides, lipids, total cells and dead cells of different EPS fractions in the fouling layers on the filter membranes, and
ii. to identify the predominant EPS compounds that determine sludge filterability.

Received 1 November 2009; accepted 31 December 2009.
Address correspondence to Duu-Jong Lee, Department of Chemical Engineering, National Taiwan University, Taipei 10617, Taiwan. Tel.: +886-2-33663028; Fax: +886-2-3363040. E-mail: djlee@ntu.edu.tw

MATERIALS AND METHODS

Samples

An excess activated sludge sample was collected from a wastewater treatment plant in the Uni-President Corp., Taiwan. This plant treats 250 m^3 of food-processing wastewater daily using primary, secondary, and tertiary treatments. The sludge pH was approximately 6.8. The chemical oxygen demand (COD) of the sludge was about 9600 mg l^{-1}, determined by a spectrometer (DR/2000; HACH, USA). The elemental composition of the dried samples was, according to an elemental analyzer (Perkin-Elmer 2400 CHN; Perkin-Elmer, country), as follows: C, 35%; H, 6%; and, N, 5%.

The supernatant was collected after the samples settled for 1.5 h at 4°C. The sediment was re-suspended to the original volume using phosphate-buffered saline (PBS) (pH 7.2) and then centrifuged at 2000×*g* for 15 min. The bulk solution was acquired as slime, representing the part that can be removed by weak centrifugation. The bottom sediment was collected and re-suspended to its original volume using the PBS buffer solution. The suspension was then centrifuged again at 5000×*g* for 15 min. The bulk solution and sediment were collected separately; the organic matter in the bulk solution was designated the LB-EPS fraction. The sediment collected was re-suspended again with the aforementioned PBS solution to its original volume and extracted using ultrasound at 20 kHz and 130 W for 30 min. The extracted solutions were then centrifuged at 20,000×*g* for 20 min. The organic matter in the bulk solution was termed TB-EPS. Each of the EPS fractions were filtered with Whatman #1 filter papers to remove the particulates, principally the pin flocs in the supernatant, slime, LB-EPS, and TB-EPS fractions.

Dead-end membrane filtration tests on the obtained supernatant, slime, LB-EPS, and TB-EPS fractions were conducted at 30 cmHg vacuum using a 0.45-μm mixed cellulose and ester membrane (Advantec MFS, Inc., CA). The membrane and the deposit layer were carefully removed from the filtration chamber under fully hydrated conditions for further processing.

Fluorescent Staining and CLSM Imaging

SYTO 63 (20 μM, 100 μl) was first added to the sample that was placed on a shaker table for 30 min. Then, 0.1 mol $NaHCO_3$ buffer (100 μl) was added to maintain the solution at pH 9, followed by adding an FITC solution (10 g l^{-1}, 10 μl), and the mixture stirred for 1 h. Next, a Con A solution (250 mg l^{-1}, 100 μl) was added to the sample for another 30 min, followed by Calcofluor White (300 mg l^{-1}, 100 μl) for 30 min, then a Nile Red solution (10 mg l^{-1}, 60 μl) for 10 min. As for each of the above-mentioned five staining stages, the sample was washed twice with the PBS solution to remove the extra stain. Finally, an SYTOX Blue solution (2.5 μM, 100 μl) was incubated with the sample for 10 min.

The stained samples were embedded for cryosectioning and were frozen at −20°C. The 30 μm sections were cut on a cryomicrotome (Cyrotome E, Thermo Shandon Limited, UK) and mounted onto the gelatin-coated (0.1% gelatin and 0.01% chromium potassium sulfate) microscopic slides for CLSM (Leica TCS SP2 confocal spectral microscope imaging system, Germany) observation. The samples were imaged with a × 10 objective and analyzed with the Leica confocal software.

Fluorescent EEM Analysis

The fluorescence excitation emission matrix (EEM) spectra of the different EPS fractions were conducted according to the procedure of Lü et al. (44). The filtered EPS fractions were further diluted to DOC less than 10 mg l^{-1} to ensure that the maximum fluorescence signal would not exceed 90% of the maximum set with the high level detection limit. Fluorescence EEM were measured on a Varian Eclipse fluorescence spectrophotometer in scan mode. EEM spectra were gathered with scanning emission (Em) spectra from 250 to 600 nm at 2 nm increments by varying the excitation (Ex) wavelength from 200 to 500 nm at 10 nm increments. The spectra were recorded at a scan rate of 1200 nm/min, using excitation and emission slit bandwidths of 5 nm. The voltage of the photomultiplier tube (PMT) was set to 800 V for low level light detection. Each scan was composed of 171 emission and 31 excitation wavelengths. The EEM of a control Milli-Q water was subtracted from each of the collected EEM.

The fluorescence regional integration (FRI) proposed by Chen et al. (45), a quantitative technique that integrates the volume beneath an EEM, was applied to characterize the nature of organic matters in different EPS fractions. The regions I, II, and IV in EEM spectra represent the tyrosine-like, tryptophan-like, and soluble microbial by-product (SMP)-like materials, respectively. The regions III and V are attributable to fulvic acid-like and humic acid-like substances.

Analytical Methods

All chemical analyses on samples were carried out in duplicate using chemicals of analytical grade. The quantity of proteins was determined by the modified Lowry method (46), using casein (Shanghai Sangon Biotechnology Co., Ltd, China) as the standard. The quantity of polysaccharides was measured by the Anthrone method (47), with glucose as the standard. The supernatant of sludge, after being filtered with 0.45-μm mixed cellulose and ester membrane (Advantec MFS, Inc., CA) was measured for DOC by a TOC/TN analyzer (multi N/C 3000, Analytik Jena AG, Germany).

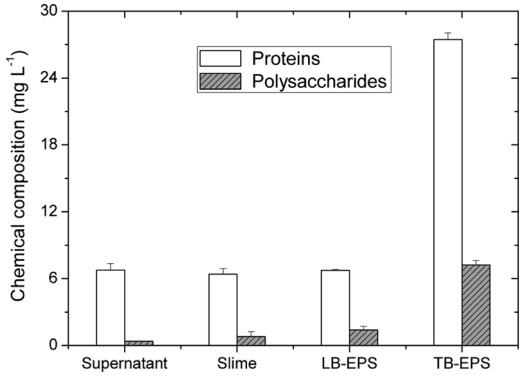

FIG. 1. Proteins and polysaccharides of different EPS fractions.

RESULTS AND DISCUSSION

Proteins and Polysaccharides of Different EPS Fractions

The contents of proteins and polysaccharides were presented in Fig. 1. It was noted that protein was predominant when compared with PS in sludge flocs. Proteins and polysaccharides were presented principally in the TB-EPS fraction ($27 \pm 1\,mg\,l^{-1}$ versus $7.2 \pm 0.4\,mg\,l^{-1}$), few in the supernatant ($6.7 \pm 0.6\,mg\,l^{-1}$ versus $0.4 \pm 0\,mg\,l^{-1}$), slime ($6.4 \pm 0.5\,mg\,l^{-1}$ versus $0.8 \pm 0.4\,mg\,l^{-1}$), LB-EPS ($6.7 \pm 0.1\,mg\,l^{-1}$ versus $1.4 \pm 0.4\,mg\,l^{-1}$). Therefore, a majority of the proteins and polysaccharides (>58%) distributed in the TB-EPS fraction, with the remainder (<42%) presented in the other three EPS fractions.

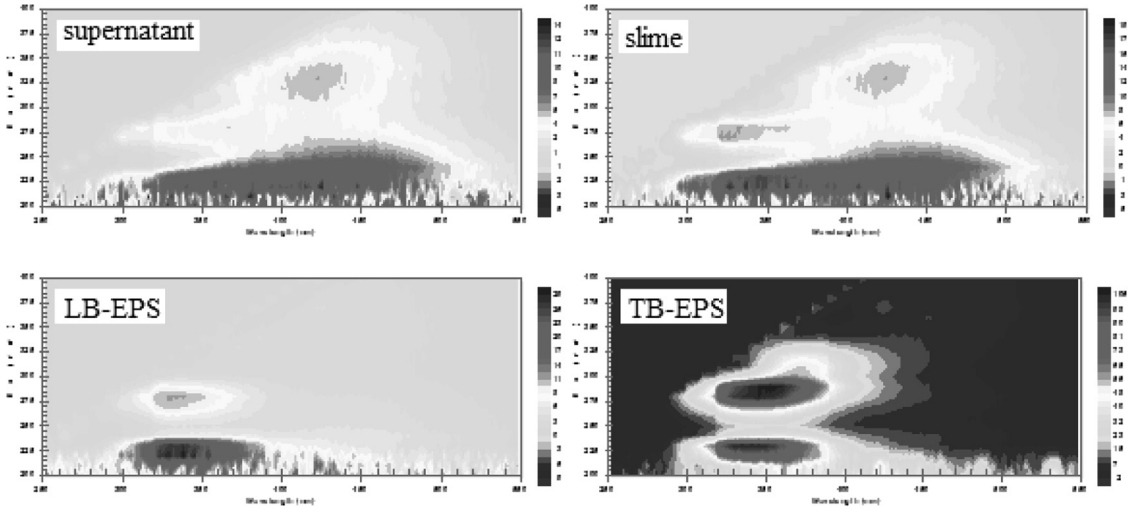

(a)

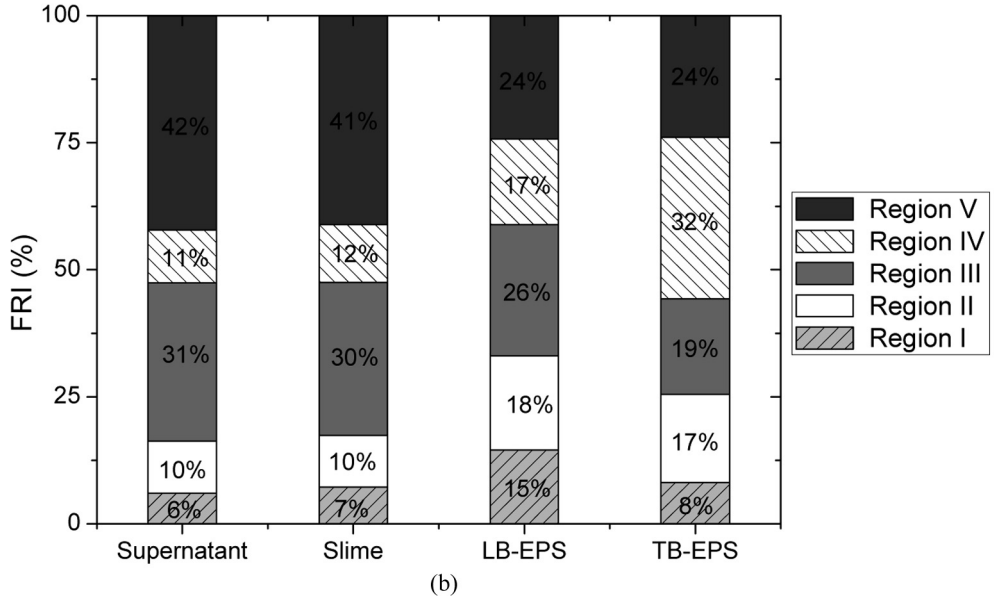

(b)

FIG. 2. EEM contour (a) and FRI analysis (b) of different EPS fractions.

FRI Analysis of Extracted EPS Fractions

The EEM contours of different EPS fractions revealed four major peaks for the supernatant and slime fractions, whereas only two peaks were noted in the LB–EPS and TB-EPS fractions (Fig. 2a). More humin-like substances and less protein-like substances were found in the supernatant and slime fractions than in the LB-EPS and TB-EPS fractions.

The FRI analysis determined that the supernatant and slime fractions had a similar but at different magnitudes FRI distributions (Fig. 2b). The humin-like substances (Region V) most contributed to the EEM spectra for these two EPS fractions, (41 – 42%), followed by fulvic-like substances (30 – 31%, Region III), SMP substances (11 – 12%, Region IV), tryptophan (10%, Region II), and tyrosine (6 – 7%, Region I). Restated, the organic matters in the

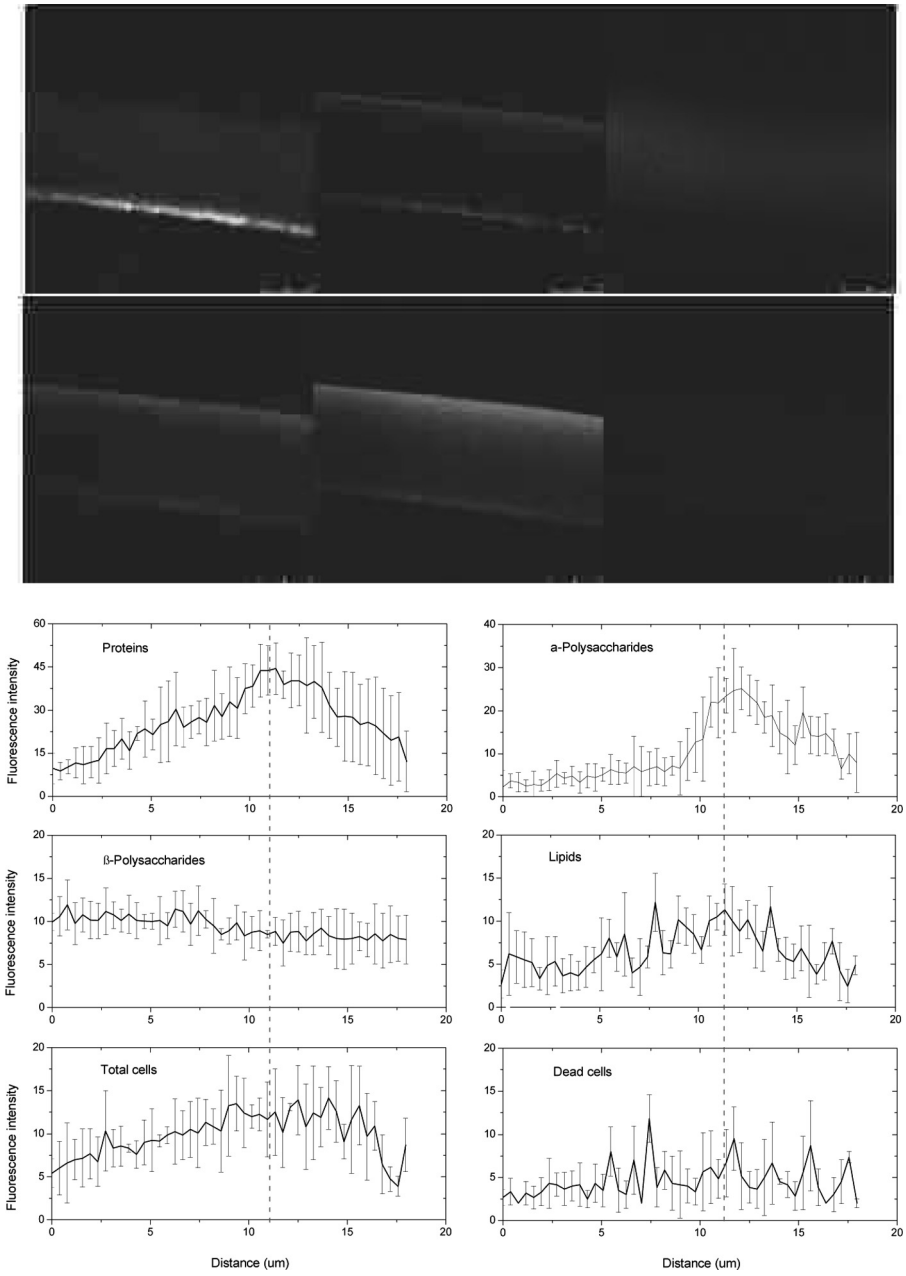

FIG. 3. CLSM side-view images of 30-μm cryosections cutting from supernatant deposit layer on filter membrane with a 10 × objective lens. Distributions of intensity alone the indicated line were shown in lower panel. Note that the left and right regions on the broken line represent the initial (compact) deposit layer and the incompact deposit layer. Error bars indicate the standard deviations of five samples. [Top panel: left, proteins; middle, α-polysaccharides; right, β-polysaccharides. Bottom panel: left, lipids; middle, total cells; right, dead cells.]

supernatant and slime fractions possessed a high degree of humification.

As for the LB-EPS fraction, however, it possessed the highest tyrosine-like (15%, Region I) and tryptophan-like (18%, Region II) signals among the four tested EPS fractions. Each of the protein-like (Region I, II, and IV) and the humin-like (Region III, and V) compounds provide about 50% of total FRI signals.

The TB-EPS fraction had a distinct FRI distribution pattern from the other three EPS fractions. The TB-EPS fraction showed the highest percentage (32%) of SMP substances (Region IV) and the lowest percentage (19%) of fulvic-like substances (Region III) among the tested EPS fractions. Meanwhile, protein-like substances (Region I, II, and IV) slightly enriched (57%) over that for humin-like (Region III and V) substances.

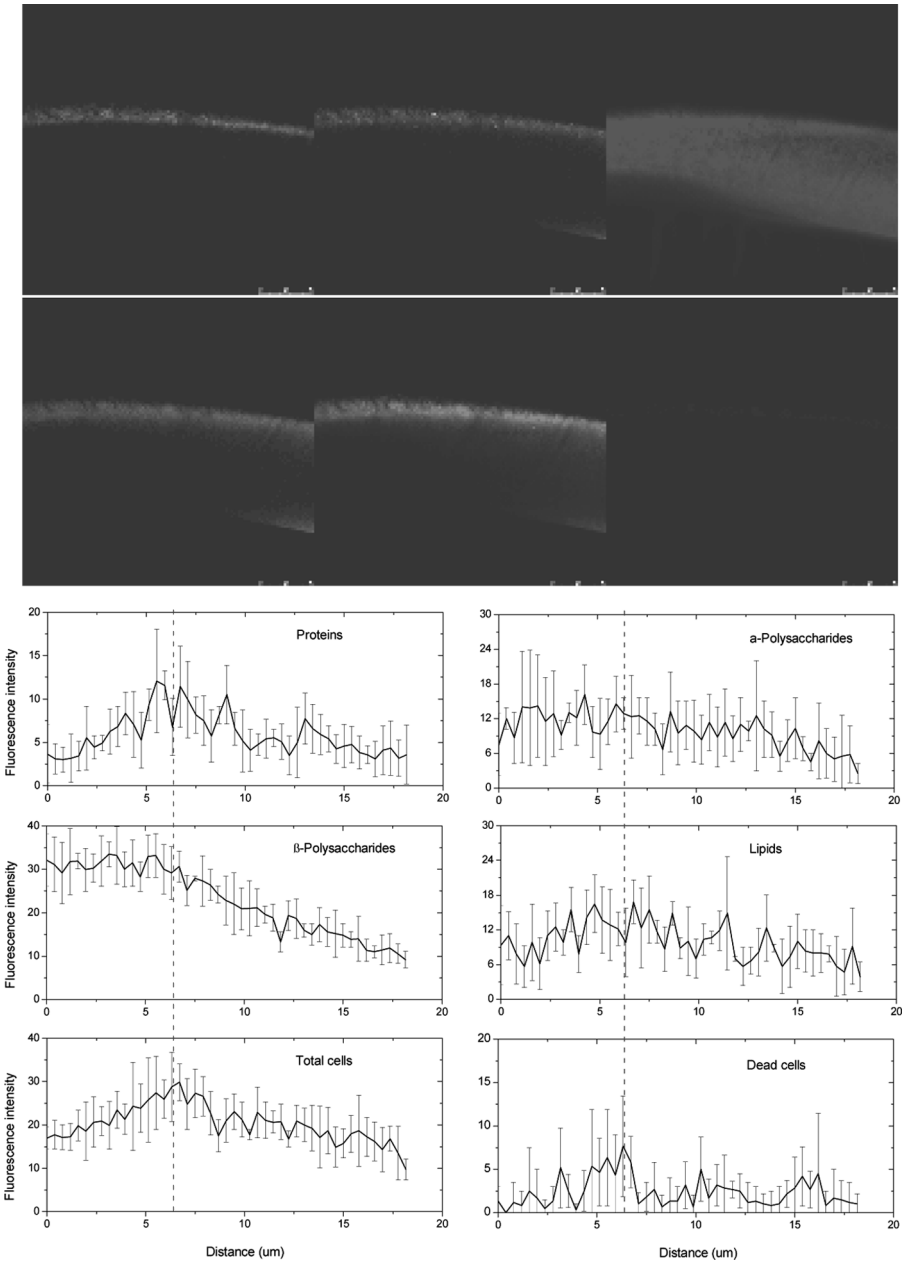

FIG. 4. CLSM side-view images of 30-μm cryosections cutting from slime deposit layer on filter membrane with a 10 × objective lens. Distributions of intensity alone the indicated line were shown in lower panel. Note that the left and right regions on the broken line represent the initial (compact) deposit layer and the incompact deposit layer. Error bars indicate the standard deviations of five samples. [Top panel: left, proteins; middle, α-polysaccharides; right, β-polysaccharides. Bottom panel: left, lipids; middle, total cells; right, dead cells.]

The FRI analysis revealed the similarities and differences among the different EPS fractions. The protein-like substances were enriched and the humin-like substances diminished when the EPS became cell-bound.

Vertical Distributions of Different EPS Fractions in Deposit Layers

CLSM side-view images in microtome of different EPS fractions and corresponding fluorescence intensity were illustrated in Figs. 3–6. The thickness of the deposit layers was about 18 μm for supernatant and slime, only 13 μm for LB-EPS, but up to 85 μm for TB-EPS. The very deep deposit layer of TB-EPS could be attributable to its high proteins content as revealed by chemical analysis and FRI analysis (Figs. 1 and 2). The homogeneous structure of the deposit layers was observed in all the deposit layers of different EPS fractions.

In the dead-end filtration test of all the tested EPS fractions, the vertical distribution of deposit layers obviously showed a two-phase characteristic, i.e., the initial

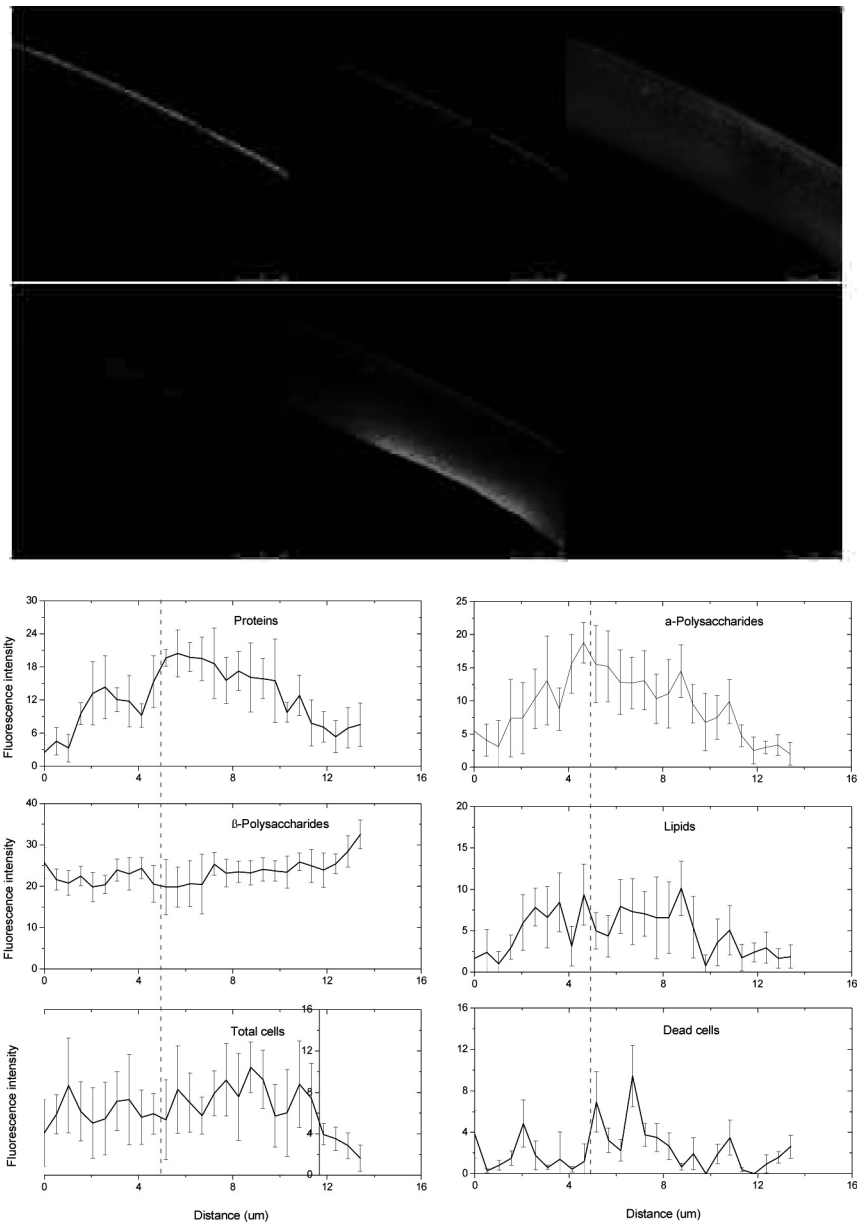

FIG. 5. CLSM side-view images of 30-μm cryosections cutting from LB-EPS deposit layer on filter membrane with a 10 × objective lens. Distributions of intensity alone the indicated line were shown in lower panel. Note that the left and right regions on the broken line represent the initial (compact) deposit layer and the incompact deposit layer. Error bars indicate the standard deviations of five samples. [Top panel: left, proteins; middle, α-polysaccharides; right, β-polysaccharides. Bottom panel: left, lipids; middle, total cells; right, dead cells.]

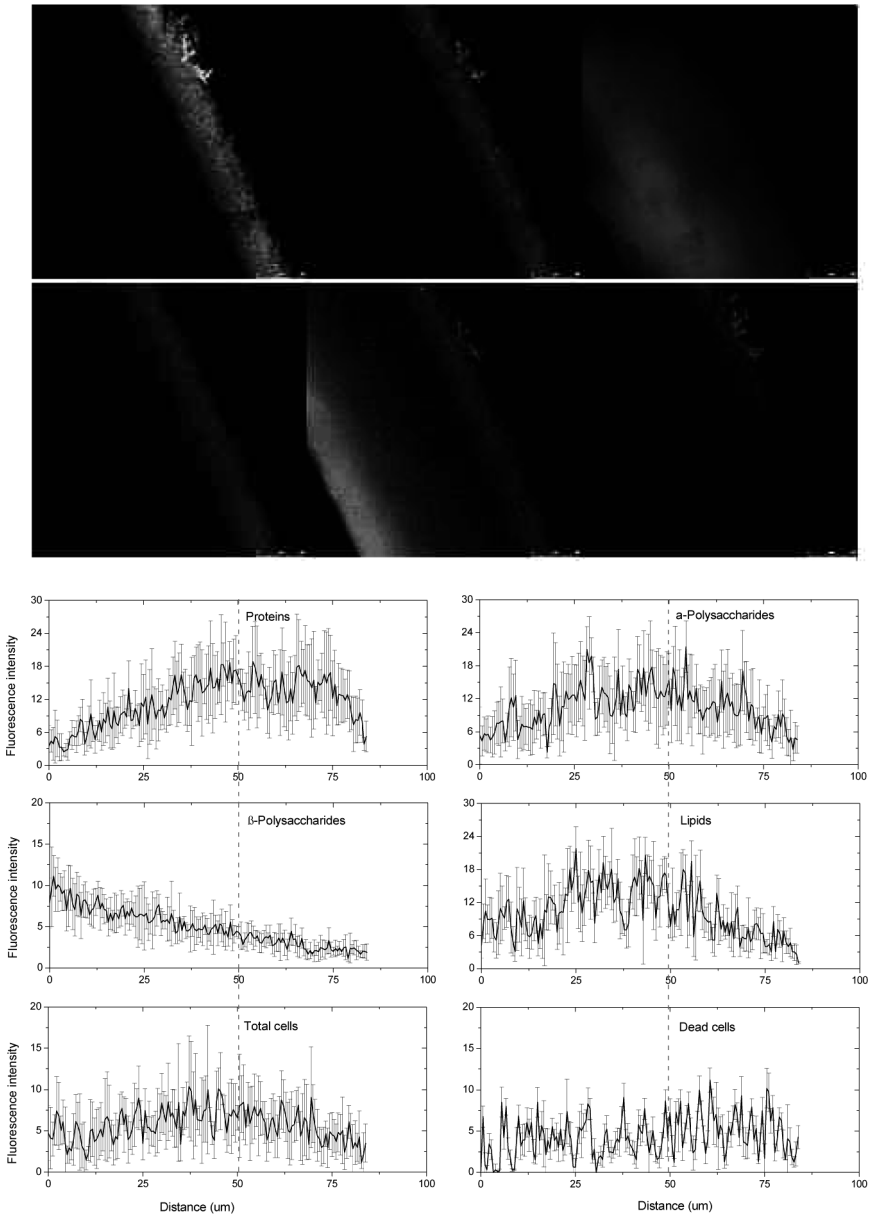

FIG. 6. CLSM side-view images of 30-μm cryosections cutting from TB-EPS deposit layer on filter membrane with a 10 × objective lens. Distributions of intensity alone the indicated line were shown in lower panel. Note that the left and right regions on the broken line represent the initial (compact) deposit layer and the incompact deposit layer. Error bars indicate the standard deviations of five samples. [Top panel: left, proteins; middle, α-polysaccharides; right, β-polysaccharides. Bottom panel: left, lipids; middle, total cells; right, dead cells.]

compact layer and the subsequent deposit layer. However, the interface distance to the membrane surface between the two layers was different. Specifically, the interface was 11 μm, 6 μm, 5 μm, and 50 μm near the membrane surface ($x = 0$) for the supernatant, slime, LB-EPS, and TB-EPS, respectively.

In the initial compact layer of the supernatant, the fluorescence intensities of proteins, α-polysaccharides, lipids, and total DNA increased with the vertical distance while the corresponding intensities for β-polysaccharides decreased slightly. On the interface, the intensities of proteins, α-polysaccharides, and lipids were about 4.6, 11, and 2.3 times higher than those at the membrane surface, respectively, suggesting that proteins, α-polysaccharides, and lipids could pass through the membrane at the beginning of filtration while the accumulation occurred with the proceed of filtration. In the subsequent deposit layer of the supernatant, however, all the fluorescence intensities of these EPS decreased gradually or leveled off (i.e., β-polysaccharides). As for dead cells, they changed slightly in the whole layer.

As for the slime deposit layer, the trends of fluorescence intensities of EPS were similar to those of the supernatant. Specifically, proteins and lipids increased about 3.3 and 1.8 times on the interface respectively while the corresponding intensities for β-polysaccharides decreased slightly. However, the fluorescence intensities of α-polysaccharides increased slightly (only by one fold). In the subsequent deposit layer of slime, all the fluorescence intensities of these EPS decreased gradually.

As for the LB-EPS deposit layer, the trends of the fluorescence intensities of EPS were also the same to those of supernatant and slime. Proteins, α-polysaccharides, and lipids were about 8.2, 3.4, and 3.9 times higher than those at the membrane surface respectively, while the corresponding intensities for β-polysaccharides changed slightly. In the subsequent deposit layer of LB-EPS, almost all the fluorescence intensities of these EPS decreased gradually, except that β-polysaccharides seemed to have increased slightly.

As for the TB-EPS deposit layer, the trends of the fluorescence intensities of EPS were similar to those of the supernatant, the slime, and the LB-EPS. Proteins, α-polysaccharides, and lipids were about 5.3, 3.3, and 4.5 times higher than those at the membrane surface respectively, while the corresponding intensities for β-polysaccharides decreased slightly. In the subsequent deposit layer of TB-EPS, all the fluorescence intensities of these EPS decreased gradually.

CLSM Images of EPS Fraction above the Membrane

Since the formed deposit layers of supernatant, slime, and LB-EPS were too thin to cryosection from the membrane surface, only CLSM images in microtome of TB-EPS deposit layer above the membrane surface were shown in Fig. 7. It seemed that proteins, α-polysaccharides, lipids, and total cells formed a continuous deposit layer, while β-polysaccharides and the dead cells were aggregated into clusters. Restated, proteins formed a more dense continuous deposit layer than α-polysaccharides, lipids, and total cells.

Proteins and polysaccharides were predominantly distributed in the TB-EPS fraction, few in the other fractions, suggesting that sludge flocs were typical and comparable to other investigations. With increase in shear force, the EPS fractions showed more protein-like and less humin-like substances. The trend of protein-like substances was

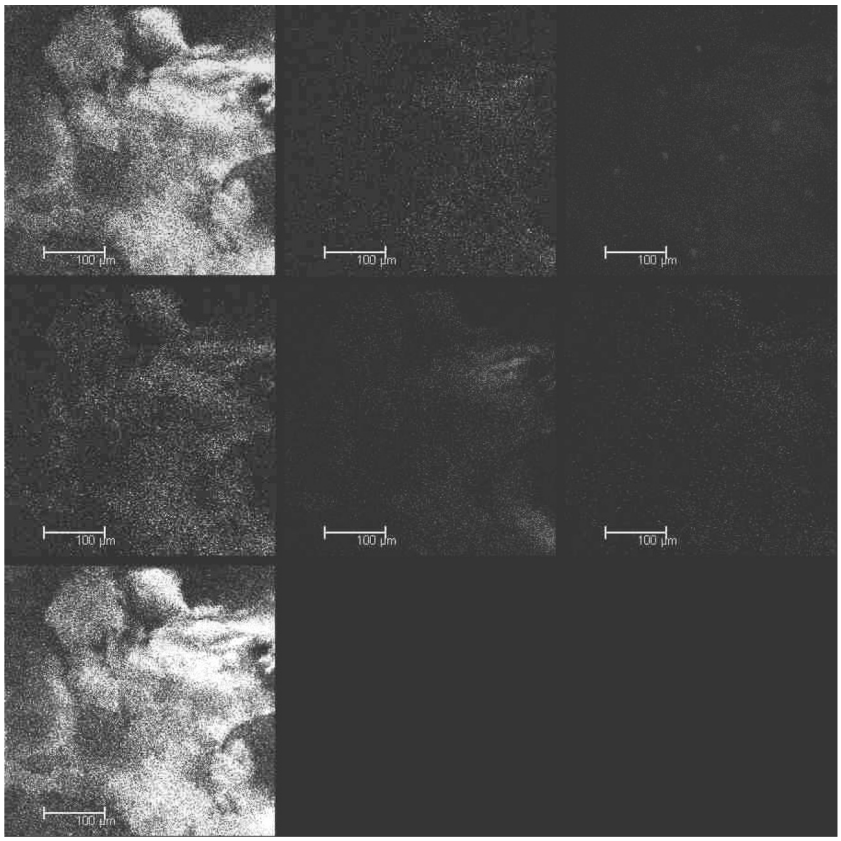

FIG. 7. CLSM images of microtome of TB-EPS deposit layer. [Top panel: left, proteins; middle, α-polysaccharides; right, β-polysaccharides. Bottom panel: left, lipids; middle, total cells; right, dead cells.]

supported by the chemical analysis (Fig. 1). The EEM contour and its FRI analysis clearly revealed the similarities and differences among the different EPS fractions. Ramesh et al. (36,37) investigated the SMP, LB-EPS, and TB-EPS of wastewater sludge by Fourier transform infrared spectra and found that they were markedly different. Tsai et al. (48) indicated that LB-EPS exhibited similar but not identical characteristics with SMP and behaved significantly differently from TB-EPS based on size exclusion chromatography and EEM fingerprint.

The vertical distribution of EPS in the deposit layer revealed that the two-phase characteristics existed, i.e., the initial compact layer and the subsequent deposit layer. The bottom layers were considerably more compact than the top deposit layer. Presumably the initial deposit layer has been compacted by the subsequent deposit layers.

Different EPS fractions had a different influence on the filterability. In the supernatant, LB-EPS and TB-EPS fractions, proteins, α-polysaccharides, and lipids affected the filterability. In the slime fraction, however, proteins and lipids rather than α-polysaccharides affected the filterability. Meanwhile, proteins had a greater impact than lipids on the filterability in all of the EPS fractions. It was also observed that β-polysaccharides were first deposited on the membrane surface. However, it was not accumulated but passed through the membrane, suggesting that β-polysaccharides had no effects on the filterability.

CONCLUSIONS

The EEM contour and FRI analysis revealed the similarities and differences among different EPS fractions extracted from activated sludge, particularly on the filterability and the fouling layer on a membrane. The FRI distribution pattern of the supernatant fraction was similar to that of the slime fraction, but was different from that of the LB-EPS and TB-EPS fractions. Protein-like substances were enriched, while the humin-like substances were diminished in the cell-bound fractions.

The different EPS fractions affect differently on the membrane filterability. In the supernatant, LB-EPS, and TB-EPS fractions, the quantities of proteins, α-polysaccharides, and lipids significantly influenced the membrane filterability. In the slime fraction, both proteins and lipids rather than α-polysaccharides affected the filterability. Meanwhile, proteins had a greater impact on the filterability than lipids in all EPS fractions. The β-polysaccharides in all the EPS fractions were not accumulated with filtration, suggesting that β-polysaccharides had no effects on filterability.

ACKNOWLEDGEMENT

This work was supported by the National Natural Science Foundation of China (No. 50876024).

REFERENCES

1. Srisukphun, T.; Chiemchaisri, C.; Yamamoto, K. (2008) Modeling of RO flux decline in textile wastewater reclamation plants using variable fouling index. *Sep. Sci. Technol.*, 43: 1704–1721.
2. Asmatulu, R. (2008) Removal of moisture from the ultra fine particles using both high centrifugal force and air pressure. *Sep. Sci. Technol.*, 43: 265–274.
3. Jiang, J.Q.; Wang, H.Y. (2008) Comparative coagulant demand of polyferric chloride and ferric chloride for the removal of humic acid. *Sep. Sci. Technol.*, 43: 386–397.
4. Zhu, H.T.; Wen, X.H.; Huang, X.; Noguchi, M.; Gan, Y.P. (2008) Membrane fouling in the reclamation of secondary effluent with an ozone-membrane hybrid system. *Sep. Sci. Technol.*, 43: 1221–130.
5. Sung, S.S.; Ju, S.P.; Hsu, C.; Mujumdar, A.S. (2008) Floc strength evaluation at alternative shearing with presence of natural organic matters. *Drying Technol.*, 26: 996–1001.
6. Ramesh, A.; Lee, D.J.; Wang, M.L.; Hsu, J.P.; Juang, R.S.; Hwang, K.J.; Liu, J.C.; Tseng, S.J. (2006) Biofouling in membrane bioreactor. *Sep. Sci. Technol.*, 41: 1345–1370.
7. Chen, M.Y.; Lee, D.J.; Tay, J.H. (2006) Extracellular polymeric substances in fouling layers. *Sep. Sci. Technol.*, 41: 1467–1474.
8. Lee, D.J.; Hsu, Y.H. (1994) Use of capillary suction apparatus for estimating the averaged specific resistance of filtration cake. *J. Chem. Technol. Biotechnol.*, 59: 45–51.
9. Chu, C.P.; Lee, D.J. (2004) Multiscale structures of biological flocs. *Chem. Eng. Sci.*, 59: 1875–1883.
10. Chen, G.W.; Chang, I.L.; Hung, W.T.; Lee, D.J. (1996) Regimes for zone settling of waste activated sludge. *Water Res.*, 30: 1844–1850.
11. Chang, I.L.; Lee, D.J. (1998) Ternary expression stage in biological sludge dewatering. *Water Res.*, 32: 905–914.
12. Chen, G.W.; Lin, W.W.; Lee, D.J. (196) Capillary suction time (CST) as a measure of sludge dewaterability. *Water Sci. Technol.*, 34: 443–448.
13. Lee, D.J.; Lee, S.F. (1995) Measurement of bound water-content in sludge – The use of differential scanning calorimetry (DSC). *J. Chem. Technol. Biotechnol.*, 62: 359–365.
14. Chen, G.W.; Hung, W.T.; Chang, I.L.; Lee, S.F.; Lee, D.J. (1997) Continuous classification of moisture content in waste activated sludge. *J. Envir. Eng. ASCE*, 123: 253–258.
15. Chang, I.L.; Chu, C.P.; Lee, D.J.; Huang, C. (1997) Polymer dose effects on filtration followed by expression of clay slurries. *J. Colloid Interf. Sci.*, 185: 335–342.
16. Le-Clech, P.; Chen, V.; Fane, A.G. (2006) Fouling in membrane bioreactors used in wastewater treatment. *J. Membr. Sci.*, 284: 17–53.
17. Chen, J.H.; Hwang, X.; Lee, D.J. (2008) Study on bisphenol A removal by a membrane bioreactor. *Process Biochem.*, 43: 451–456.
18. Baker, J.S.; Dudley, L.Y. (1998) Biofouling in membrane systems—a review. *Desalination*, 118: 81–90.
19. Judd, S. (2004) A review of fouling of membrane bioreactors in sewage treatment. *Water Sci. Technol.*, 492: 229–235.
20. Judd, S. (2005) Fouling control in submerged membrane bioreactors. *Water Sci. Technol.*, 51: 27–34.
21. Marrot, B.; Barrios-Martinez, A.; Moulin, P.; Roche, N. (2004) Industrial wastewater treatment in a membrane bioreactor: A review. *Envir. Prog.*, 23: 59–68.
22. Liao, B.Q.; Bagley, D.M.; Kraemer, H.E.; Leppard, G.G.; Liss, S.N. (2004) A review of biofouling and its control in membrane separation bioreactors. *Water Envir. Res.*, 76: 425–436.
23. Ramesh, A.; Lee, D.J.; Wang, M.L.; Hsu, J.P.; Juang, R.S.; Hwang, K.J.; Liu, J.C.; Tseng, S.T. (2006) Biofouling in membrane bioreactor. *Sep. Sci. Technol.*, 41: 1345–1370.
24. Huang, X.; Liu, R.; Qian, Y. (2000) Behavior of soluble microbial products in a membrane bioreactor. *Process Biochem.*, 36: 401–406.

25. Nagaoka, H.; Ueda, S.; Miya, A. (1996) Influence of bacterial extracellular polymers on the membrane separation activated sludge process. *Water Sci. Technol.*, 34: 165–172.
26. Wang, X.M.; Li, X.Y. (2008) Accumulation of biopolymer clusters in a submerged membrane bioreactor and its effect on membrane fouling. *Water Res.*, 42: 855–862.
27. Sun, F.Y.; Wang, X.M.; Li, X.Y. (2008) Visualisation and characterisation of biopolymer clusters in a submerged membrane bioreactor. *J. Membr. Sci.*, 325: 691–697.
28. Wisniewski, C.; Grasmick, A. (1998) Floc size distribution in a membrane bioreactor and consequences for membrane fouling. *Colloid Surf. A*, 138: 403–411.
29. Bouhabila, E.H.; Aim, R.B.; Buisson, H. (2001) Fouling characterization in membrane bioreactors. *Sep. Purif. Technol.*, 22/23: 123–132.
30. Defrance, L.; Jaffrinm, M.Y.; Gupta, B.; Paullier, P.; Geaugey, V. (2000) Contribution of various species present in activated sludge to membrane bioreactor fouling. *Bioresour. Technol.*, 73: 105–112.
31. Bouhabila, E.H.; Ben Aim, R.; Buisson, H. (2001) Fouling characterization in membrane bioreactors. *Sep. Purif. Technol.*, 22–23: 123–132.
32. Barker, D.J.; Stuckey, D.C. (1999) A review of soluble microbial products (SMP) in wastewater treatment systems. *Water Res.*, 33: 3063–3082.
33. Jarusutthirak, C.; Amy, G.; Croue, J.P. (2002) Fouling characteristics of wastewater effluent organic matter (EfOM) isolates on NF and UF membranes. *Desalination*, 145: 247–255.
34. Jarusutthirak, C.; Amy, G. (2007) Understanding soluble microbial products (SMP) as a component of effluent organic matter (EfOM). *Water Res.*, 41: 2787–2793.
35. Howe, K.J.; Clark, M.M. (2002) Fouling of microfiltration and ultrafiltration membranes by natural waters. *Environ. Sci. Technol.*, 36: 3571–3576.
36. Ramesh, A.; Lee, D.J.; Hong, S.G. (2006) Soluble microbial products (SMP) and soluble extracellular polymeric substances (EPS) from wastewater sludge. *Appl. Microb. Biotechnol.*, 73: 219–225.
37. Ramesh, A.; Lee, D.J.; Lai, J.Y. (2007) Membrane biofouling by extracellular polymeric substances or soluble microbial products from membrane bioreactor sludge. *Appl. Microb. Biotechnol.*, 74: 699–704.
38. Yu, G.H.; He, P.J.; Shao, L.M.; He, P.P. (2008) Stratification structure of sludge flocs with implications to dewaterability. *Environ. Sci. Technol.*, 42: 7944–7949.
39. Yu, G.H.; He, P.J.; Shao, L.M.; Lee, D.J. (2008) Extracellular enzymes in sludge flocs collected at fourteen full-scale wastewater treatment plants. *J. Chem. Technol. Biotechnol.*, 83: 1717–1725.
40. Houghton, J.I.; Quarmby, J.; Stephenson, T. (2001) Municipal wastewater sludge dewaterability and the presence of microbial extracellular polymer. *Water Sci. Technol.*, 44: 373–379.
41. Novak, J.T.; Sadler, M.E.; Murthy, S.N. (2003) Mechanisms of floc destruction during anaerobic and aerobic digestion and the effect on conditioning and dewatering of biosolids. *Water Res.*, 37: 3136–3144.
42. Rosenberger, S.; Evenblij, H.; te Poele, S.; Wintgens, T.; Laabs, C. (2005) The importance of liquid phase analyses to understand fouling in membrane assisted activated sludge processes—Six case studies of different European Research Groups. *J. Membr. Sci.*, 263: 113–126.
43. Chen, M.Y.; Lee, D.J.; Tay, J.H. (2007) Distribution of extracellular polymeric substances in aerobic granules. *Appl. Microbiol. Biotechnol.*, 73: 1463–1469.
44. Lü, F.; Zhang, H.; Chang, C.H.; Lee, D.J.; He, P.J.; Shao, L.M.; Su, A. (2008) Dissolved organic matter and estrogenic potential of landfill leachate. *Chemosphere*, 72: 1381–1386.
45. Chen, W.; Westerhoff, P.; Leenheer, J.A.; Booksh, K. (2003) Fluorescence excitation–emission matrix regional integration to quantify spectra for dissolved organic matter. *Environ. Sci. Technol.*, 37: 5701–5710.
46. Frølund, B.; Keiding, K.; Nielsen, P. (1995) Enzymatic activity in the activated sludge flocs matrix. *Appl. Microbiol. Biotechnol.*, 43: 755–761.
47. Gaudy, A.F. (1962) Colorimetric determination of protein and carbohydrate. *Indust. Wat. Wastes*, 7: 17–22.
48. Tsai, B.N.; Chang, C.H.; Lee, D.J. (2008) Fractionation of soluble microbial products (SMP) and soluble extracellular polymeric substances (EPS) from wastewater sludge. *Environ. Technol.*, 29: 1127–1138.